Trajectory Tracking of a Quadrotor with Disturbance Rejection using Extended State Observer

2020 IEEE Asia-Pacific Conference on Computer Science and Data Engineering (CSDE) | 978-1-6654-1974-1/20/$31.00 ©2020 IEEE | DOI: 10.1109/CSDE50874.2020.9411639

Izzuddin Mat Lazim
Department of Electrical & Electronic Engineering,
Faculty of Engineering & Built Environment,
Universiti Sains Islam Malaysia,
N. Sembilan, Malaysia
nh.izzuddin@usim.edu.my

Liyana Ramli
Department of Electrical & Electronic Engineering,
Faculty of Engineering & Built Environment,
Universiti Sains Islam Malaysia,
N. Sembilan, Malaysia
lyanaramli@usim.edu.my

Abdul Rashid Husain
Division of Control and Mechatronics Engineering,
School of Electrical Engineering,
Faculty of Engineering,
Universiti Teknologi Malaysia
Johor Darul Takzim, Malaysia
abrashid@utm.my

Aminurrashid Noordin
Department of Electrical Engineering Technology,
Faculty of Electrical and Electronic Engineering Technology,
Universiti Teknikal Malaysia Melaka
Melaka, Malaysia
aminurrashid@utem.edu.my

Mus'ab Sahrim
Department of Electrical & Electronic Engineering,
Faculty of Engineering & Built Environment,
Universiti Sains Islam Malaysia,
N. Sembilan, Malaysia
musab@usim.edu.my

Ahmad 'Athif M. Faudzi
Division of Control and Mechatronics Engineering,
School of Electrical Engineering,
Faculty of Engineering,
Universiti Teknologi Malaysia
Johor Darul Takzim, Malaysia
athif@utm.my

***Abstract*— The presence of external disturbances such as wind may affect the stability of a quadrotor during flight. This paper proposes a robust autonomous flight control of a feedback linearized quadrotor model with the presence of external disturbances by using the active anti-disturbance control (AADC) technique. In the inner-loop control, the feedback linearization technique is used to simplify the nonlinear and under-actuated quadrotor dynamics into the corresponding linear representation. In the outer-loop control, the AADC technique using extended state observer (ESO) and state feedback is proposed for trajectory tracking and disturbance rejection control of the quadrotor, respectively. Here, ESO estimates the external disturbances by using only the output of the system. To evaluate the effectiveness of the proposed controller, simulations of the quadrotor were carried in which the results obtained show the advantage of the proposed control algorithm for hovering and trajectory tracking of the quadrotor.**

Keywords*— *Quadrotor, unmanned aerial vehicle, disturbance observer, extended state observer

I. Introduction

Recently, unmanned aerial vehicles (UAV) such as quadrotor has received considerable attention for various tasks including crop monitoring, surveillance, border patrol, as well as photography, and videography. Nevertheless, control of a quadrotor is nontrivial due to the underactuated and nonlinear model, and also susceptible to external disturbances such as wind. Thus, an advanced controller is needed to accomplish the designated task effectively.

A straightforward control approach for the quadrotor is by using linear controllers. In the literature, linear control such as linear quadratic regulator (LQR) and proportional-integral-derivative (PID) was proposed [1]–[3]. These linear controllers were derived based on the linearized quadrotor model around certain nominal operation conditions, e.g. hovering condition. Thus, the performance guarantee of a quadrotor using these controllers is limited around this nominal operation condition only.

Feedback linearization (FL) is another linearization approach for the quadrotor. In contrast to the linearization at an operating point only, FL produces a linear representation of the nonlinear quadrotor model over a wide range of operating conditions via coordinate transformation and nonlinear state feedback [4]. The linear representation can be used to design various linear controllers in the outer-loop control. A static FL was applied by Mahmood and Kim [5] to linearize the nonlinear quadrotor dynamics for the formation control problem. Similarly, dynamic FL was implemented in other studies to solve the trajectory tracking problem of a quadrotor [6]–[8]. However, only ideal conditions were considered in these studies in which all parameters were assume known, and no disturbance was present.

To improve the robustness of the feedback linearized model, common control methods used are adaptive and robust techniques [9], [10]. Nevertheless, the closed-loop transient response is shaped by the robust and adaptive control component instead of the nominal model. Also, these methods may not respond fast enough when a strong disturbance is present [11]. The active anti-disturbance control (AADC) technique is proposed in many studies to overcome these limitations.

Unlike adaptive or robust techniques, AADC reacts directly to the disturbance by feedforward compensation control design using sensor measurement or disturbance estimation. A high-order sliding mode observer was proposed by Mokhtari *et al.* [12] for trajectory tracking of a quadrotor in the existence of sinusoidal disturbances. More recently, a linear disturbance observer (LDO) was successfully implemented in [13], [14] to improve the robustness of FL towards wind disturbances. However, full state information is required to implement the observer. In another work, an extended state observer (ESO) was successfully employed by Liu *et al.* [15] to remove the lumped disturbance for feedback linearized rotor-active magnetic bearings. Unlike LDO that can only estimate the disturbance, ESO can also estimate the plant dynamics based on the output of the system.

Motivated by these studies, this paper aims to improve the robustness of the feedback linearized quadrotor model for solving trajectory tracking problem under the influence of external disturbance using ESO. Here, state feedback (SF) control and ESO, so-called SF-ESO are applied in the outer-loop control for trajectory tracking and disturbance rejection of the linearized quadrotor model, respectively. We show that the proposed SF-ESO can enhance the trajectory tracking performance of the quadrotor despite the occurrence of external disturbances. To the best of our knowledge, this study is the first to propose SF and ESO for improving the feedback linearized quadrotor system.

This paper is organized as follows. First, in Section II, the quadrotor dynamics is presented. Then, the proposed control system design is presented in Section III. Results and discussion are developed in Section IV. Finally, Section V concludes this paper.

II. NONLINEAR QUADROTOR MODEL

Consider a quadrotor configuration seen in Fig. 1 with $\mathbb{F}_e = \{x_e, y_e, z_e\}$ is the earth-fixed frame, $\mathbb{F}_b = \{x_b, y_b, z_b\}$ is the body-fixed frame, and F_j ($j = 1,2,3,4$) are the lift forces produced by the four rotors. Let $\{x, y, z\}$ denotes the absolute position of the quadrotor with respect to $\mathbb{F}_e$, and $\{\phi, \theta, \psi\}$ denotes the orientation (roll, pitch, yaw) of the quadrotor. By considering the translational and rotation components, the 6-DOF dynamic model of the quadrotor can be expressed as [5]

$$\ddot{x} = \alpha\, u^{\{1\}}/m + T_x/m \quad (1)$$

$$\ddot{y} = \beta\, u^{\{1\}}/m + T_y/m \quad (2)$$

$$\ddot{z} = -a_g + \gamma\, u^{\{1\}}/m + T_z/m \quad (3)$$

$$\ddot{\phi} = \dot{\theta}\dot{\psi}\left(I_y - I_z\right)/I_x + u^{\{2\}}/I_x \quad (4)$$

$$\ddot{\theta} = \dot{\phi}\dot{\psi}\left(I_z - I_x\right)/I_y + u^{\{3\}}/I_y \quad (5)$$

$$\ddot{\psi} = \dot{\phi}\dot{\theta}\left(I_x - I_y\right)/I_z + u^{\{4\}}/I_z \quad (6)$$

where $\boldsymbol{u} = \left[u^{\{1\}}, u^{\{2\}}, u^{\{3\}}, u^{\{4\}}\right]^T$ are the control inputs of the system, m is the mass of quadrotor, a_g is the gravitational acceleration, and

$$\begin{aligned} \alpha &= c(\phi)s(\theta)c(\psi) + s(\phi)s(\psi) \\ \beta &= c(\phi)s(\theta)s(\psi) - s(\phi)c(\psi) \\ \gamma &= c(\phi)c(\theta) \end{aligned} \quad (7)$$

with the terms $s(\cdot)$ and $c(\cdot)$ are the sine and cosine functions, respectively. Meanwhile T_q and I_q $(q = x, y, z)$ denote the disturbing forces on the quadrotor and the moment of inertia along each axis, respectively.

The quadrotor dynamic is underactuated and nonlinear as can be seen from (1) - (6) which may create a challenge in the controller design process. One of the approaches to solve this issue is by linearizing the dynamics via the FL method as presented in the following section.

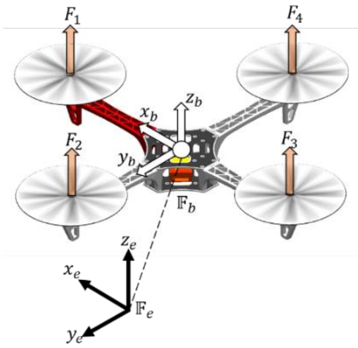

Fig. 1. The configuration of a quadrotor.

III. CONTROL SYSTEM DESIGN

This section presents the proposed control algorithm that allows the quadrotor to track the desired trajectory while simultaneously rejecting the external disturbances which present in the quadrotor dynamics in (1) - (6). The control algorithm consists of inner-loop control and outer-loop control. FL technique is used in the inner-loop control to simplify the nonlinear and underactuated quadrotor dynamics into four linear-decoupled equations. For the outer-loop control, linear state-feedback control is designed for trajectory tracking based on the assumption that the inner-loop control is linear. To improve the tracking control, the ESO is employed to estimate the lumped disturbance on the quadrotor. A detail of the proposed control algorithm is presented in the following subsections.

A. Feedback Linearization of Quadrotor Dynamics

Linearization of nonlinear dynamics via feedback linearization approach involves coordinate transformation and nonlinear state feedback [4]. In this study, the absolute position of the quadrotor (x, y, z) and heading (ψ) are selected as the output to be controlled. Since the quadrotor dynamics is underactuated in which $\ddot{x}, \ddot{y}$ and $\ddot{z}$ in (1) - (6) are all depend on $u^{\{1\}}$, control input $u^{\{1\}}$ need to be delayed by double integrator while other control inputs remain unchanged [16]. For notation consistency, control input $\boldsymbol{u} = \left[u^{\{1\}}, u^{\{2\}}, u^{\{3\}}, u^{\{4\}}\right]^T$ are replaced by $\bar{\boldsymbol{u}} = \left[\bar{u}^{\{1\}}, \bar{u}^{\{2\}}, \bar{u}^{\{3\}}, \bar{u}^{\{4\}}\right]^T$, i.e.

$$\begin{aligned} &\bar{u}^{\{1\}} = \dot{\xi},\ \ \dot{\zeta} = \xi,\ \ \zeta = u^{\{1\}} \\ &\bar{u}^{\{2\}} = u^{\{2\}} \\ &\bar{u}^{\{3\}} = u^{\{3\}} \\ &\bar{u}^{\{4\}} = u^{\{4\}} \end{aligned} \quad (8)$$

By considering control input $\bar{\boldsymbol{u}}$, dynamics in (1) - (6) can be written as

$$\begin{aligned} \dot{\mathbf{x}} &= \mathbf{f}(\mathbf{x}) + \sum_{j=1}^{4} \mathbf{g}_j\,(\mathbf{x})\bar{u}^{\{j\}} \\ \mathbf{y} &= [h_1, h_2, h_3, h_4]^T = [x, y, z, \psi]^T \end{aligned} \quad (9)$$

In which $\mathbf{x} = \left[p_x, \dot{p}_x, p_y, \dot{p}_y, p_z, \dot{p}_z, \zeta, \xi, \phi, \dot{\phi}, \theta, \dot{\theta}, \psi, \dot{\psi}\right]^T \in \mathbb{R}^{14}$ is the extended state, $\mathbf{y}$ is the output vector, and

$$\mathbf{f}(\mathbf{x}) = \left[\dot{p}_x, \frac{(\alpha\zeta + T_x)}{m}, \dot{p}_y, \frac{(\beta\zeta + T_y)}{m}, \dot{p}_z, -a_g + \frac{(\gamma\zeta + T_z)}{m}, \xi, 0, \dot{\phi}, \frac{\dot{\theta}\dot{\psi}(I_y - I_z)}{I_x}, \dot{\theta}, \frac{\dot{\phi}\dot{\psi}(I_z - I_x)}{I_y}, \dot{\psi}, \frac{\dot{\psi}\dot{\theta}(I_x - I_y)}{I_z}\right]^T,$$

$$\mathbf{g}_1 = [0,0,0,0,0,0,0,1,0,0,0,0,0,0]^T,$$

$$\mathbf{g}_2 = \left[0,0,0,0,0,0,0,0,0,\frac{1}{I_x},0,0,0,0\right]^T,$$

$$\mathbf{g}_3 = \left[0,0,0,0,0,0,0,0,0,0,0,\frac{1}{I_y},0,0\right]^T,$$

$$\mathbf{g}_4 = \left[0,0,0,0,0,0,0,0,0,0,0,0,0,\frac{1}{I_z}\right]^T$$

The dynamics of the quadrotor in (9) is feedback linearizable using an inner-loop control given as

$$\bar{\boldsymbol{u}} = \boldsymbol{\Delta}^{-1}(\mathbf{x})(-\mathbf{b}(\mathbf{x}) + \mathbf{v}) \tag{10}$$

where $\mathbf{v} = [v_x, v_y, v_z, v_\psi]^T$ is the vector of control input for the linearized system, and

$$\boldsymbol{\Delta} = \begin{bmatrix} \frac{\alpha}{m} & \frac{\zeta\Gamma}{mI_x} & \frac{\zeta\gamma c\psi}{mI_y} & -\frac{\zeta\beta}{mI_z} \\ \frac{\beta}{m} & -\frac{\zeta\Lambda}{mI_x} & \frac{\zeta\gamma s\psi}{mI_y} & \frac{\zeta\alpha}{mI_z} \\ \frac{\gamma}{m} & -\frac{\zeta s\phi c\theta}{mI_x} & -\frac{\zeta c\phi s\theta}{mI_y} & 0 \\ 0 & 0 & 0 & \frac{1}{I_z} \end{bmatrix} \tag{11}$$

$$\mathbf{b}(\bar{x}) = \begin{bmatrix} L_f^{r_1} h_1(\mathbf{x}) \\ \vdots \\ L_f^{r_4} h_4(\mathbf{x}) \end{bmatrix} \tag{12}$$

with $\Gamma = c\phi s\psi - s\phi s\theta c\psi$ and $\Lambda = c\phi c\psi + s\phi s\theta s\psi$. $L_g^k h_j$ denotes the k-th Lie derivative of h_j along g. In case of exact feedback linearization with no external disturbances, i.e. $T_x = T_y = T_z = 0$, (10) transforms the quadrotor dynamics in eq. (9) into four decoupled linear dynamics given as

$$\frac{d(\ddot{x})}{dt} = v_x, \quad \frac{d(\ddot{y})}{dt} = v_y, \quad \frac{d(\ddot{z})}{dt} = v_z, \quad \frac{d(\dot{\psi})}{dt} = v_\psi \tag{13}$$

However, exact feedback linearization may not be possible in practice as there are always parameter uncertainties and external disturbances on the quadrotor dynamics, i.e. $T_q \neq 0$ $(q = x, y, z)$. Thus, inexact feedback linearization occurs which yield nominal linear part and the unknown disturbance part, $\mathbf{d} = [d_x, d_y, d_z, d_\psi]^T$ given by

$$\frac{d(\ddot{x})}{dt} = v_x + d_x, \quad \frac{d(\ddot{y})}{dt} = v_y + d_y, \quad \frac{d(\ddot{z})}{dt} = v_z + d_z, \quad \frac{d(\dot{\psi})}{dt} = v_\psi + d_\psi \tag{14}$$

B. ESO Design

Consider $w_1 = [x, y, z]^T$ and $w_6 = \psi$. Then, the linearized dynamics (14) is transformed into the extended-state equation given as

$$\begin{aligned} \dot{w}_1 &= w_2 \\ \dot{w}_2 &= w_3 \\ \dot{w}_3 &= w_4 \\ \dot{w}_4 &= w_5 + [v_1, v_2, v_3]^T \\ \dot{w}_5 &= [\dot{d}_x, \dot{d}_y, \dot{d}_z]^T \end{aligned} \tag{15}$$

$$\begin{aligned} \dot{w}_6 &= w_7 \\ \dot{w}_7 &= w_8 + v_4 \\ \dot{w}_8 &= \dot{d}_\psi \end{aligned} \tag{16}$$

To estimate the disturbance $\dot{d}_j$ $(j = x, y, z, \psi)$, a linear ESO is designed as [11]

$$\begin{aligned} \dot{\hat{w}}_1 &= \hat{w}_2 - \beta_1(\hat{w}_1 - w_1) \\ \dot{\hat{w}}_2 &= \hat{w}_3 - \beta_2(\hat{w}_1 - w_1) \\ \dot{\hat{w}}_3 &= \hat{w}_4 - \beta_3(\hat{w}_1 - w_1) \\ \dot{\hat{w}}_4 &= \hat{w}_5 - \beta_4(\hat{w}_1 - w_1) + [v_1, v_2, v_3]^T \\ \dot{\hat{w}}_5 &= -\beta_5(\hat{w}_1 - w_1) \end{aligned} \tag{17}$$

$$\begin{aligned} \dot{\hat{w}}_6 &= \hat{w}_7 - \beta_6(\hat{w}_6 - w_6) \\ \dot{\hat{w}}_7 &= \hat{w}_8 - \beta_7(\hat{w}_6 - w_6) + v_4 \\ \dot{\hat{w}}_8 &= -\beta_8(\hat{w}_6 - w_6) \end{aligned} \tag{18}$$

where $\hat{w}_1, \hat{w}_2, \dots, \hat{w}_8$ are estimates of states $w_1, w_2, \dots, w_8$, respectively, and $\beta_1, \beta_1, \dots, \beta_8$ are the observer gains to be designed. Note that the disturbances are estimated by the extended states, i.e.

$$\begin{aligned} \hat{w}_5 &= [\hat{d}_x, \hat{d}_y, \hat{d}_z]^T \\ \hat{w}_8 &= \hat{d}_\psi \end{aligned} \tag{19}$$

Proposition 1: For a bounded disturbance $\dot{d}_j$, there exist observer gains $\beta_1, \beta_1, \dots, \beta_8$ such that the ESO (18) renders $(\hat{w}_1, \hat{w}_2, \dots, \hat{w}_8) \to (w_1, w_2, \dots, w_8)$.

Proof: Subtracting (15) - (16) from (17) - (18), the observer error is given by

$$\begin{aligned} \dot{e}_1 &= e_2 - \beta_1 e_1 \\ \dot{e}_2 &= e_3 - \beta_2 e_1 \\ \dot{e}_3 &= e_4 - \beta_3 e_1 \\ \dot{e}_4 &= e_5 - \beta_4 e_1 \\ \dot{e}_5 &= -\beta_5 e_1 - [\dot{d}_x, \dot{d}_x, \dot{d}_x]^T \end{aligned} \tag{20}$$

$$\begin{aligned} \dot{e}_6 &= e_7 - \beta_6 e_6 \\ \dot{e}_7 &= e_8 - \beta_7 e_6 \\ \dot{e}_8 &= -\beta_8 e_6 - \dot{d}_\psi \end{aligned} \tag{21}$$

where $e_i = \hat{w}_i - w_i$ $(i = 1,2,..8)$ represents the estimation error. It has been shown that BIBO stability for (20) is guaranteed under the assumption that $\dot{d}_j$ is bounded [11]. The observer gains can be determined by using the pole placement method, where the characteristic equations for (20) - (21) are given by [15]

$$\left(s+\omega_q\right)^5=0 \tag{22}$$

$$\left(s+\omega_\psi\right)^3=0 \tag{23}$$

where ω_q and ω_ψ are positive bandwidth values. Then, the ESO gains are calculated as

$$\begin{aligned}&\beta_1=5\omega_q, \beta_2=10\omega_q^2\\&\beta_3=10\omega_q^3, \beta_4=5\omega_q^4\\&\beta_5=\omega_q^5\end{aligned} \tag{24}$$

$$\beta_6=3\omega_\psi, \beta_7=3\omega_\psi^2, \beta_8=\omega_\psi^3 \tag{25}$$

This concludes the proof. ■

C. Closed-loop Controller Design

The feedback linearized model in (14) can be written in a state-space form as

$$\dot{\mathbf{w}}_j=\mathbf{A}_j\mathbf{w}_j+\mathbf{B}_j\left(v_j+d_j\right) \quad j\in\{x,y,z,\psi\} \tag{26}$$

with $\mathbf{w}_q=[q,\dot{q},\ddot{q},\dddot{q}]^T$ $(q=x,y,z)$ and $\mathbf{w}_\psi=[\psi,\dot{\psi}]^T$, and

$$\begin{aligned}&\mathbf{A}_x=\mathbf{A}_y=\mathbf{A}_z=\begin{bmatrix}0&1&0&0\\0&0&1&0\\0&0&0&1\\0&0&0&0\end{bmatrix},\\&\mathbf{A}_\psi=\begin{bmatrix}0&1\\0&0\end{bmatrix},\\&\mathbf{B}_x=\mathbf{B}_y=\mathbf{B}_z=[0\ 0\ 0\ 1]^T,\\&\mathbf{B}_\psi=[0\ 1]^T\end{aligned}$$

A classical state-feedback (SF) controller can be implemented in the outer-loop control to track the desired trajectory and stabilize (26) given by

$$v_{o_j}=-\mathbf{K}_j\mathbf{w}_j+G_jR_j, \quad j\in\{x,y,z,\psi\} \tag{27}$$

with $\mathbf{K}_j$, G_j, and R_j represent the feedback gain matrix, feedforward gain, and desired output trajectory, respectively. The closed-loop dynamics is obtained by substituting (27) into (26), given as

$$\dot{\mathbf{w}}_j=\left(\mathbf{A}_j-\mathbf{B}_j\mathbf{K}_j\right)\mathbf{w}_j+G_j\mathbf{B}_jR_j+\mathbf{B}_jd_j \tag{28}$$

The closed-loop dynamics in (28) is influenced by the external disturbance d_j . To improve the control, a compensation scheme by integrating SF and ESO, so-called SF-ESO is designed in this paper, given by

$$v_j=v_{o_j}-\hat{d}_j \tag{29}$$

where v_{o_j} is the nominal SF in (27), while $\hat{d}_j$ is the estimated disturbance in (19). Substituting (29) into (26) yields

$$\begin{aligned}\dot{\mathbf{w}}_j&=\left(\mathbf{A}_j-\mathbf{B}_j\mathbf{K}_j\right)\mathbf{w}_j+G_j\mathbf{B}_jR_j+\mathbf{B}_j\left(d_j-\hat{d}_j\right)\\&=\left(\mathbf{A}_j-\mathbf{B}_j\mathbf{K}_j\right)\mathbf{w}_j+G_j\mathbf{B}_jR_j+\mathbf{B}_je_j\end{aligned} \tag{30}$$

where $e_j=d_j-\hat{d}_j$. Based on Proposition 1, $e_j=0$ which indicates that the external disturbance is effectively rejected by the controller.

IV. Results and Discussion

In this section, the performance of the proposed SF-ESO is evaluated by implementing the algorithm in a MATLAB/Simulink simulation environment. The quadrotor model parameters are adopted from [5] with $m=0.6$ kg, $I_x=0.005796\ \mathrm{kg\cdot m^2}$, $I_y=0.005796\ \mathrm{kg\cdot m^2}$, $I_z=0.010296\mathrm{kg\cdot m^2}$ and $a_g=9.81\mathrm{ms^{-2}}$. For the feedback control, state feedback gains are $\mathbf{K}_x=\mathbf{K}_y=\mathbf{K}_z=[81\ 108\ 54\ 12]$, and $\mathbf{K}_\psi=[6\ 9]$ which were chosen based on the pole-placement method. For estimating and compensating the lumped disturbance in the translational axis, the gain for ESO is $\omega_q=70$. Meanwhile for yaw, no ESO is used as the disturbance is not considered as in (6). Initially, the quadrotor is assumed to be on ground at coordinate $[x(0),y(0),z(0)]=[0,0,0]m$ with heading of $\psi(0)=\pi/2rad$. Other states were set to zero.

Two simulation studies were carried out to test the effectiveness of the proposed control algorithm towards rejecting external disturbances. The bounded external disturbances considered which may represent wind disturbances and parameter uncertainties are given as [17]

$$\begin{aligned}T_x=T_y&=5\sin 0.5t+2\sin 0.5t\\&\quad+2\sin\left(2t+\frac{\pi}{2}\right)\\&\quad+\sin\left(3t-\frac{\pi}{3}\right)\\T_z&=3\sin(1.5t)+2\sin(0.5t)\\&\quad+0.2\sin\left(t+\frac{\pi}{2}\right)\end{aligned} \tag{31}$$

The simulation results are presented in the following subsections. The performance of the proposed SF-ESO is compared with the classical state feedback control (SF) that has no disturbance rejection capability as a benchmark given in (27). Integral absolute error (*IAE*) is used to quantify the controllers' performance given as

$$IAE=\int_0^{\mathcal{T}}|E(t)|dt \tag{32}$$

Here, $\mathcal{T}$ is the simulation period and $E=r_q-q,(q=x,y,z,\psi)$ is the error between the desired and actual value.

A. Simulation Experiment 1: Hover

Hover is one of the main maneuvers of a quadrotor which is important for various missions in which the quadrotor needs to remain in one place. In this simulation work, the quadrotor supposed to fly from the initial position on the ground to the desired hovering position and heading given by

$$\begin{aligned}&\left[R_x,R_y,R_z\right]=[1,-1,2]m\\&\psi(0)=\pi/2rad\end{aligned} \tag{33}$$

The ability of the quadrotor to hover at this fixed position despite the presence of external disturbances in (31) is studied in this simulation experiment. The proposed controller in (29) was implemented to achieve this objective. The performance of the proposed controller is compared with the results obtained by using SF as a benchmark. The results of this simulation experiment are shown in Fig. 2 and tabulated in TABLE I.

In Fig. 2, the time response of the quadrotor for hovering maneuver by using SF and SF-ESO controller is shown. Generally, both controllers were able to make the quadrotor fly to the desired fixed position. Nevertheless, some deviations from hover position can be seen in the translational motion (x,y,z) for the quadrotor with SF which was caused by the external disturbances.

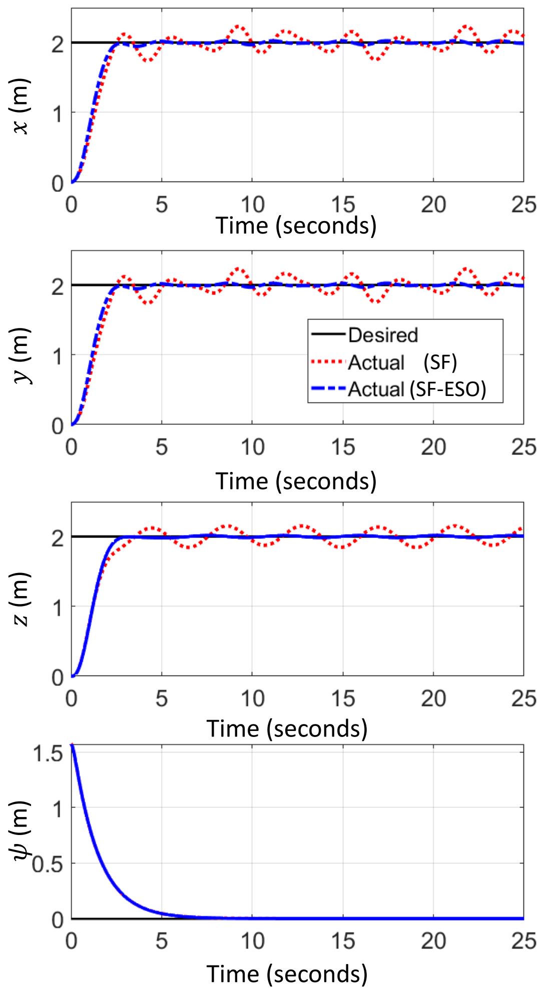

Fig. 2. Time response of the hovering quadrotor.

On the contrary, a good hover control can be seen by the quadrotor with SF-ESO which is shown by the ability to maintain the hover position despite the presence of external disturbances. This shows the ability of the proposed SF-ESO to actively reject the disturbance as further verified by quantitative analysis using *IAE* that is lower than the benchmark (SF) as tabulated in TABLE I. Notice that the performance of both controllers for heading ψ was identical as no aerodynamic moment disturbance considered.

TABLE I. QUANTITATIVE COMPARISON BETWEEN SF-DOBC AND SF-IDOBC FOR QUADROTOR HOVERING PROBLEM.

Controller	*IAE*			
	x	y	z	ψ
SF	7.2145	7.2064	7.0082	2.3562
SF-ESO	3.1051	3.1027	2.9901	2.3562
Reduction (%)	56.9603	56.9452	57.3343	0

B. Simulation Experiment 2: Time-varying Trajectory Tracking

Another important maneuver for the quadrotor is the time-varying trajectory tracking. The capability of the proposed control scheme to track the desired time-varying trajectory while rejecting the external disturbances were demonstrated in this simulation study. The desired trajectory was a circle of radius $5m$ at $2m$ above ground given as

$$\begin{aligned} R_x(t) &= 5\sin(0.1257t) \\ R_y(t) &= 5\sin\left(0.1257t + \frac{\pi}{2}\right) \\ R_z(t) &= 2 \\ R_\psi(t) &= 0 \end{aligned} \quad (34)$$

In this simulation study, the external disturbances were also generated by using (31). Results of the simulation by using the proposed control (SF-ESO) and the benchmark control (SF) are shown in Fig. 3 and tabulated in TABLE II for a period of $T = 50s$.

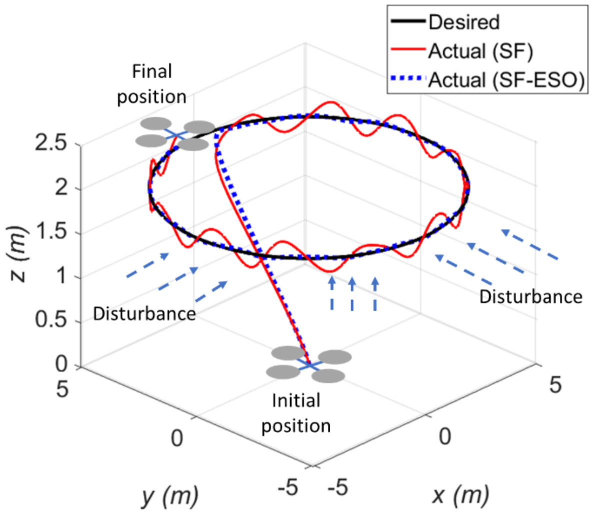

Fig. 3. 3D position for trajectory tracking of the quadrotor.

It can be seen from Fig. 3 that both controllers were generally able to track the desired circular trajectory. However, the quadrotor with the benchmark controller (SF) was struggling to closely track the desired path due to the existence of external disturbances as indicated by the large oscillation in its trajectory. In contrast, the quadrotor with the proposed SF-ESO was able to closely track the desired circular path while rejecting the external disturbances as shown by the smooth trajectory. This is further supported by quantitative analysis via the *IAE* performance index tabulated in TABLE II that shows some reduction in the error which was achieved by the proposed SF-ESO with respect to the benchmark SF.

TABLE II. QUANTITATIVE COMPARISON BETWEEN SF-DOBC AND SF-IDOBC FOR QUADROTOR HOVERING PROBLEM.

Controller	*IAE*			
	x	y	z	ψ
SF	25.9657	32.8302	7.0059	2.3562
SF-ESO	25.6592	32.4668	2.9891	2.3563
Reduction (%)	1.1804	1.1069	57.3345	0

V. Conclusion

An active disturbance rejection control scheme is proposed in this paper to improve the robustness of autonomous trajectory tracking of a quadrotor in the presence of external disturbances. This is achieved by using SF and ESO that respectively track the desired trajectory and compensate for the lumped disturbance of inexact feedback linearized quadrotor system. Two simulation studies were carried out: hovering and trajectory tracking of the quadrotor in the presence of bounded time-varying disturbances. Results show that the proposed controller improves the hovering and trajectory tracking of the quadrotor as compared to the benchmark controller. Future research direction includes the deployment of the proposed controller on experimental hardware.

ACKNOWLEDGMENT

The authors would like to thank Universiti Sains Islam Malaysia (USIM) for supporting this research under the USIM-RACER Research Grant No. PPPI/USIM-RACER_0120/FKAB/051000/12920.

REFERENCES

[1] A. L. Salih, M. Moghavvemi, H. A. F. Mohamed, and K. S. Gaeid, “Modelling and PID controller design for a quadrotor unmanned air vehicle,” in *2010 IEEE International Conference on Automation Quality and Testing Robotics (AQTR)*, 2010, vol. 1, pp. 1–5.

[2] T. Sangyam, P. Laohapiengsak, W. Chongcharoen, and I. Nilkhamhang, “Path tracking of UAV using self-tuning PID controller based on fuzzy logic,” in *Proceedings of SICE Annual Conference 2010*, 2010, pp. 1265–1269.

[3] A. Dharmawan, T. K. Priyambodo, and others, “Model of Linear Quadratic Regulator (LQR) Control Method in Hovering State of Quadrotor,” *J. Telecommun. Electron. Comput. Eng.*, vol. 9, no. 3, pp. 135–143, 2017.

[4] M. A. Henson and D. E. Seborg, “Feedback linearizing control,” in *Nonlinear process control*, no. 1, Upper Saddle River, NJ, USA: Prentice-Hall, Inc., 1997, pp. 149–232.

[5] A. Mahmood and Y. Kim, “Leader-following formation control of quadcopters with heading synchronization,” *Aerosp. Sci. Technol.*, vol. 47, pp. 68–74, 2015.

[6] V. Mistler, A. Benallegue, and N. K. M’Sirdi, “Exact linearization and noninteracting control of a 4 rotors helicopter via dynamic feedback,” in *Proceedings 10th IEEE International Workshop on Robot and Human Interactive Communication*, 2001, pp. 586–593.

[7] F. Sabatino, “Quadrotor control : modeling, nonlinear control design, and simulation,” KTH Royal Institute of Technology, 2015.

[8] A. Mahmood and Y. Kim, “Decentralized formation control of quadcopters using feedback linearization,” in *International Conference on Automation, Robotics and Applications*, 2015, pp. 537–541.

[9] I. H. Choi and H. C. Bang, “Quadrotor-tracking controller design using adaptive dynamic feedback-linearization method,” *Proc. Inst. Mech. Eng. Part G J. Aerosp. Eng.*, vol. 228, no. 12, pp. 2329–2342, 2014.

[10] W. Zhao and T. H. Go, “Quadcopter formation flight control combining MPC and robust feedback linearization,” *J. Franklin Inst.*, vol. 351, no. 3, pp. 1335–1355, 2014.

[11] S. Li, J. Yang, W. H. Chen, and X. Chen, *Disturbance observer-based control: methods and applications*. Boca Raton, Florida: CRC Press, 2014.

[12] A. Mokhtari, N. K. M’Sirdi, K. Meghriche, and A. Belaidi, “Feedback linearization and linear observer for a quadrotor unmanned aerial vehicle,” *Adv. Robot.*, vol. 20, no. 1, pp. 71–91, 2006.

[13] A. Aboudonia, A. El-Badawy, and R. Rashad, “Disturbance observer-based feedback linearization control of an unmanned quadrotor helicopter,” *Proc. Inst. Mech. Eng. Part I J. Syst. Control Eng.*, vol. 230, no. 9, pp. 877–891, 2016.

[14] I. M. Lazim, A. R. Husain, N. A. M. Subha, and M. A. M. Basri, “Intelligent Observer-Based Feedback Linearization for Autonomous Intelligent Observer-Based Feedback Linearization for Auton- omous Quadrotor Control,” *Int. J. Eng. Technol.*, vol. 7, no. 4.35, pp. 904–911, 2018.

[15] C. Liu, G. Liu, and J. Fang, “Feedback Linearization and Extended State Observer-Based Control for Rotor-AMBs System With Mismatched Uncertainties,” *IEEE Trans. Ind. Electron.*, vol. 64, no. 2, pp. 1313–1322, Feb. 2017.

[16] H. Wang and M. Chen, “Sliding mode attitude control for a quadrotor micro unmanned aircraft vehicle using disturbance observer,” in *Proceedings of 2014 IEEE Chinese Guidance, Navigation and Control Conference*, 2014, pp. 568–573.

[17] I. M. Lazim, A. R. Husain, Z. Mohamed, M. A. M. Basri, N. A. M. Subha, and L. Ramli, “Disturbance observer-based formation tracking control of multiple quadrotors in the presence of disturbances,” *Trans. Inst. Meas. Control*, vol. 41, no. 14, pp. 4129–4141, 2019.